MedChemComm

Accepted Manuscript

This is an *Accepted Manuscript*, which has been through the Royal Society of Chemistry peer review process and has been accepted for publication.

Accepted Manuscripts are published online shortly after acceptance, before technical editing, formatting and proof reading. Using this free service, authors can make their results available to the community, in citable form, before we publish the edited article. We will replace this *Accepted Manuscript* with the edited and formatted *Advance Article* as soon as it is available.

You can find more information about *Accepted Manuscripts* in the Information for Authors.

Please note that technical editing may introduce minor changes to the text and/or graphics, which may alter content. The journal's standard Terms & Conditions and the Ethical guidelines still apply. In no event shall the Royal Society of Chemistry be held responsible for any errors or omissions in this *Accepted Manuscript* or any consequences arising from the use of any information it contains.

ROYAL SOCIETY OF CHEMISTRY

www.rsc.org/medchemcomm

Journal Name

RSCPublishing

ARTICLE

Photoswitching property of hairpin ODNs with azobenzene derivatives in the loop

Cite this: DOI: 10.1039/x0xx00000x

Li Wu,[a,b] Ya Wu,[c] Hongwei Jin,*[b] Liangren Zhang,[b] Yujian He,*[a,b] and Xinjing Tang*[b]

Received 00th January 2012,
Accepted 00th January 2012

DOI: 10.1039/x0xx00000x

www.rsc.org/

We report herein a possibility of modulating the structure of hairpin oligonucleotides (ODNs) with light. By using 4.4′-dihydroxyl azobenzene derivatives as suitable linker units, the hairpin conformation can be photocontrolled in a reversible manner. To determine which cross-links show the largest photoswitching effect, 4,4'-bis(hydroxymethyl)azobenzene (**Az1**) and 4,4'-bis(hydroxyethyl)azobenzene (**Az2**) were designed and replaced with loops of ODN hairpins. When **Az1** was introduced as the loop of ODN hairpins with 4, 5 and 6 base pairs, thermodynamic stability of the ODN hairpins decreased and the differences in T_m values from *trans* to *cis* were 12.1-24.1 °C, whereas this did not happen for **Az2**-ODN hairpins. CD results indicated that the azobenzene modified hairpins displayed strong induced CD signals at the range of 300-350 nm and 400-450 nm. Thermodynamic parameters showed that the enthalpic change ($-\Delta H^o$) and the entropic decrease ($-T\Delta S^o$) for *trans* to *cis* isomerization of **Az1**-ODN **5a**, **6a** and **8a** significantly decreased with a decrease in T_m values, whereas $-\Delta H^o$ and $-T\Delta S^o$ for **Az2**-ODN **5b** and **6b** clearly increased in spite of little change in T_m values. Quantum chemical calculation further explained that the stabilities of *trans*-form are much higher than their *cis* form for **Az1**-ODNs, but not for **Az2**-ODNs.

Introduction

Nucleic acids are ideal building blocks for construction of nano-devices and regulation of gene expression by the highly sequence-specific hybridization of complementary sequences. Strategic incorporation of photoresponsive molecules into nucleic acids potentially provides a powerful strategy for modulating their structural and functional properties in time and space. The ability to transform biomolecules from one unique structure into another one on demand, for instance, could be exploited to spatiotemporally control gene expression,[1-6] remotely detect cell signaling,[7] trigger nano-machines,[8-10] regulate protein folding[11] or manipulate enzyme activities.[12-14] Approaches for photocaged nucleic acids with photolabile groups,[2, 4, 6] and light initiated nucleic acid cross-linking[15, 16] have been recently developed. Azobenzene compounds, may undergo a reversible change in their structures and properties, have attracted most attentions in the field of nano materials and biological applications.[17-20]

Three generally applicable aspects have been developed to modify nucleic acids with azobenzene moieties. First, many published works are based on photoregulation of nucleic acids with the intercalation of azobenzene derivatives.[21-23] Second, modifications with monofuctional azobenzene moieties (e.g., interference with ligand binding) have been employed for modulating oligonucleotide duplex and triplex formation and DNA transcription.[24-28] However, introducing a single cross-linker in nucleic acid led to little switch effect. Finally, modifications with bifunctional azobenzene moieties are intended to induce the largest structural rearrangement and thereby change activity of the target. For example, bifuctional azobenzene derivatives had been used to cross-link peptides in a highly specific manner, and conformations and activities of these chemically modified peptides or proteins can be modulated in a reversible manner by irradiation.[29, 30] Furthermore, bifunctional modification at the 4, 4′-positions of azobenzene was also achieved by introducing azobenzene moieties in oligonucleotides, whereas the structural switch induced by light exposure were seldom reported.[31-33] Previously, a dihydroxy functional cross linker with azobenzene moieties was introduced to the loop oligonucleotide in a single five bp ODN hairpin and was able to reversibly control the whole hairpin stability via UV or visible light irradiation.[5]

In this study, 4,4'-bis(hydroxymethyl)azobenzene (**Az1**) and 4,4'-bis(hydroxyethyl)azobenzene (**Az2**) were developed as switching element of ODN hairpin at the loop position to evaluate the effect of photoresponsive azobenzene linker on the structure and

[a]*College of Chemistry and Chemical Engineering, University of Chinese Academy of Sciences, Beijing 100049, China. Email: heyujian@ucas.ac.cn*
[b]*State Key Laboratory of Natural and Biomimetic Drugs, School of Pharmaceutical Sciences, Peking University, Beijing 100191, China. E-mail: jinhw@bjmu.edu.cn; xinjingt@bjmu.edu.cn*
[c]*College of Chemistry and Chemical Engineering, Xi'an Shiyou University, Xi'an 710062, China.*

† Electronic supplementary information (ESI) available: melting temperature, native PAGE, UV spectra, typical UV melting curves, CD spectra, thermoisomerization behavior and mass spectrum. See DOI: 10.1039/b000000x/

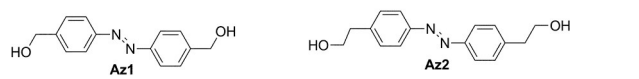

1a: 5'-GGAC**Az1**GTCC-3'	**1b**: 5'-GGAC**Az2**GTCC-3'	**1c**: 5'-GGAC**TTTT**GTCC-3'
2a: 5'-GATC**Az1**GATC-3'	**2b**: 5'-GATC**Az2**GATC-3'	**2c**: 5'-GATC**TTTT**GATC-3'
3a: 5'-AAAG**Az1**CTTT-3'	**3b**: 5'-AAAG**Az2**CTTT-3'	**3c**: 5'-AAAG**TTTT**CTTT-3'
4a: 5'-AAAAG**Az1**CTTTT-3'	**4b**: 5'-AAAAG**Az2**CTTTT-3'	**4c**: 5'-AAAAG**TTTT**CTTTT-3'
5a: 5'-AATAG**Az1**CTATT-3'	**5b**: 5'-AATAG**Az2**CTATT-3'	**5c**: 5'-AATAG**TTTT**CTATT-3'
6a: 5'-AATAC**Az1**GTATT-3'	**6b**: 5'-AATAC**Az2**GTATT-3'	**6c**: 5'-AATAC**TTTT**GTATT-3'
7a: 5'-AATAA**Az1**TTATT-3'	**7b**: 5'-AATAA**Az2**TTATT-3'	**7c**: 5'-AATAA**TTTT**TTATT-3'
8a: 5'-AATAT**Az1**ATATT-3'	**8b**: 5'-AATAT**Az2**ATATT-3'	**8c**: 5'-AATAT**TTTT**ATATT-3'
9a: 5'-AAAAA**Az1**TTTTT-3'	**9b**: 5'-AAAAA**Az2**TTTTT-3'	**9c**: 5'-AAAAA**TTTT**TTTTT-3'
10a: 5'-AAAAAA**Az1**TTTTTT-3'	**10b**: 5'-AAAAAA**Az2**TTTTTT-3'	**10c**: 5'-AAAAAA**TTTT**TTTTTT-3'

Figure 1 Structures of 4,4'-bis(hydroxymethyl)azobenzene (**Az1**) and 4,4'-bis(hydroxyethyl)azobenzene (**Az2**), and ODN sequences used in the study.

activity of hairpin ODNs. Different combinations of self-complementary hairpin ODNs with four, five and six different base pairs as the stem of oligonucleotides were used, as shown in Figure 1. Here, the factors that change the thermostabilities of hairpins were investigated, including the length of the polyA-polyT sequences, the content of GC bases, the base pair neighbouring to azobenzene in stem of hairpins. Our intent was to explore the generality of the stem structural switch and learn more about the secondary structure between *trans* and *cis* state. We found a general decrease in thermostability from *trans* to *cis* state for 4,4'-bis(hydroxymethyl)azobenzene whereas no decrease for 4,4'-bis(hydroxyethyl)azobenzene. The optimized structures of *trans*-form and *cis*-form determined by molecular dynamics simulation agreed well with the higher thermodynamic stability of *trans*-conformation for **Az1** linked hairpins than their *cis*-conformation. These results further suggested that the predicted azobenzene linker unit was very important for hairpin switching on/off and thus will became promising for the applications as a photo-induced DNA modulator based on its unique photo-switching property. We further applied light-induced structural change of azobenzene to analyze how the predicted secondary structure of these hairpins is involved in *trans* and *cis* state.

Results and discussion

Synthesis, structure and thermodynamic stability

Trans-**Az1** and **Az2** phosphoramidites were synthesized according to a previous report,[5] and were then incorporated in a series of ODNs by standard phosphoramide chemistry on an automated DNA synthesizer. The sequences of all ODNs used are shown as Figure 1.

It was previously reported that DNA duplex instead of DNA hairpin was formed by introduction of 3,3'-bis(hydroxymethyl)azobenzene in oligonucleotides for on/off regulation.[34] Differently, by increasing the concentration of azobenzene modified ODNs, no obvious changes of melting temperature (T_m) for both **Az1**- and **Az2**-ODNs were observed (Figure S1), which indicated their T_m values were independent of ODN concentrations and they possibly formed hairpin structures instead of double-stranded duplexes. We further confirmed ODN hairpin formation using native PAGE gel. As shown in Figure 2, azobenzene modified ODN **1a**, **1b**, **4a** and **4b** showed the identical or similar mobility to their corresponding natural hairpin ODN with

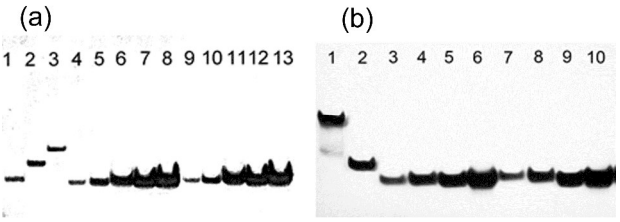

Figure 2. Native polyacrylamide gel electrophoresis pattern. **(a)** Lane1: hairpin marker, 5'-GGACTTTTGTCC-3' (**1c**), Lane2: duplex marker (9 bp), 5'-GCCGTACTG-3'/5'-CAGTACGGC-3', Lane3: duplex marker (12bp), 5'-GCCGTTTTACTG-3'/5'-CAGTAAAACGGC-3', Lane4: [**1a**] = 4 μM, Lane5: [**1a**] = 10 μM, Lane6: [**1a**] = 40 μM, Lane7: [**1a**] = 80 μM, Lane8: [**1a**] =120 μM, Lane9: [**1b**] = 4 μM, Lane10: [**1b**] = 10 μM, Lane11: [**1b**] = 40 uM, Lane12: [**1b**] = 80 μM, Lane13: [**1b**] = 120 μM. **(b)** Lane1: duplex marker (12bp), 5'-ACTGAGGACCTA-3'/5'-TAGGTCCTCAGT-3', Lane2: hairpin marker, 5'-AAAAGTTTTCTTTT-3' (**4c**), Lane3: [**4a**] = 4 μM, Lane4: [**4a**] = 10 μM, Lane5: [**4a**] = 40 μM, Lane6: [**4a**] = 120 μM, Lane7: [**4b**] = 4 μM, Lane8: [**4b**] = 10 μM, Lane9: [**4b**] = 40 μM, Lane10: [**4b**] = 120 μM.

increasing concentrations (4–120 μM). In addition, even 10 fold amount of azobenzene modified ODNs (100 μM) were loaded in the same native gel, we still found that the ODN bands were aligned in the same positions as the low concentration (10 μM) of corresponding ODNs, as shown in Figure S2, In addition, native PAGE gel showed the bands for *cis* state of azobenzene linked ODNs ran faster than their *trans* state (Figure S3), suggesting no formation of double-stranded duplex for both states of azobenzene linked ODNs. It is difficult to completely convert trans azobenzene to its *cis* form, because the energy of trans conformation is relatively high. In our case, when *trans*-**1a** after UV-light irradiation for 20 min was analyzed with HPLC, HPLC analysis further make clear that *trans*-Az1 ODN convert to its *cis* form and the conversion ratio from trans to cis was calculated to 79.8 % from the peak area (Figure s4).

Since azobenzene linkers were used as replacement of hairpin loop, it is reasonable to compare thermostability of the azobenzene modified ODN hairpins with their corresponding natural ODN hairpins. Four nucleotide loops with four thymidine nucleobases are thought to be the optimum length for natural loops in ODN hairpins. The average melting temperatures of ODNs **1a-10a**, **1b-10b**, **1c-10c** in 10 mM phosphate buffer (pH 7.0) containing 100 mM NaCl and 0.1 mM EDTA were listed in Table 1. The T_m values of the

Table 1. Melting temperatures for azobenzene-linked ODNs and their corresponding natural DNA hairpins.[a]

Az1- ODN	T_m/°C	**Az2-** ODN	T_m/°C	Hairpin	T_m/°C
1a	74.0±1.4	**1b**	70.7±1.7	**1c**	60.5±0.9
2a	63.0±1.0	**2b**	62.7±1.2	**2c**	46.2±0.6
3a	55.2±2.1	**3b**	46.0±0.5	**3c**	29.8±1.3
4a	57.5±2.0	**4b**	49.7±0.9	**4c**	39.8±0.5
5a	54.2±0.1	**5b**	49.9±0.5	**5c**	32.7±0.7
6a	56.7±0.2	**6b**	56.5±0.6	**6c**	42.1±1.0
7a	42.3±0.2	**7b**	36.5±0.4	**7c**	27.2±0.3
8a	46.6±0.3	**8b**	42.2±0.5	**8c**	28.3±0.4
9a	55.1±1.4	**9b**	48.6±2.0	**9c**	34.5±0.7
10a	57.2±0.9	**10b**	51.7±1.1	**10c**	42.6±0.2

[a] Values for 2-120 μM conjugates in 10 mM phosphate buffer containing 100 mM NaCl and 0.1 mM Na_2EDTA.

azobenzene modified ODN **1a-10a** and **1b-10b** were much higher than their corresponding natural ODN **1c-10c**, and the T_m values for **Az1**-ODN hairpin **1a-10a** were slightly higher than those for **Az2**-ODN hairpin **1b-10b**. Similar to stilbene-linked hairpins,[35, 36] *trans*-azobenzene is suggested to be stacked with closing base pair of stem duplex and the longer ethylene linker weakens the stacking interaction. The T_m values for **10a** versus **9a**, **10b** versus **9b** increased by 2.4 °C and 1.1 °C with increasing length of the polyA-polyT sequence. The T_m values for both **1a-3a** and **1b-3b** also increased with increasing the content of GC nucleobases. ODN **4a-6a** and **4b-6b** contained one neighbouring G:C base pair and thus their T_m values were higher than that of their corresponding hairpin **7a-9a** and **7b-9b** with one neighbouring A:T base pair. This may reflect a strong interaction of azobenzene with an adjacent G:C basepair than with A:T pair, which referred to similar crystallographic structure of stilbene-linked hairpin.[35]

trans to *cis* photoisomerization of azobenzene linked hairpin ODNs

Without UV illumination, azobenzene moiety exists dominantly in *trans*-form due to its thermodynamically more stable conformation in *trans* form rather than *cis*-form.[37, 38] Here, the azobenzene moity in ODNs mostly (>95%) took a *trans* form, as indicated by the UV-visible spectra and the reversed-phase HPLC.[5] The absorption spectra of *trans* form of **Az1** and **Az2** as well as **3a** and **3b** in 3:7 MeOH/H_2O were shown in Figure S5. **Az1** and **Az2** linkers displayed three typical absorption bands at 410-480 nm (n-π*), 300-380 nm (π-π*) and 230-250 nm (σ-σ*). Both azobenzene linked ODN **3a** and **3b** had similar spectra except for an absorption peak at near 260 nm, which assigned to overlapping azobenzene and nucleobase absorption band. The absorbance of **3a** and **3b** performed a slightly red-shift at wavelength of π-π* transition relative to that of **Az1** and **Az2** linker. In addition, the sample solutions containing **Az1**- and **Az2**-ODNs were irradiated in 10 mM phosphate buffer using 4W handy UV lamp (365 nm). The absorption spectra of **5a** and **5b** with UV irradiation were shown in Figure 3. The absorbance peaks at around 340 nm for **5a** and **5b** displayed a clear decrease with increasing irradiation time, whereas the 440 nm band appeared a slight increase. This indicated that *trans* to *cis* isomerization effectively proceed with UV irradiation at the wavelength of the π-π* transition for both **Az1** linked ODN **5a** and **Az2** linked ODN **5b**. Furthermore, **Az1**-ODN **5a** reached a photostationary state in 40 min with UV irradiation, while it took only 20 min for **Az2**-ODN **5b** to reach the equilibrium. The relative lower conversion speed of **Az1**-ODNs may reflect a higher internal barrier due to the interaction of azobenzene moiety and the nearby base pairs. Similarly, the absorption of the other Az1 linked ODNs with UV irradiation showed the similar variation (Figure S6).

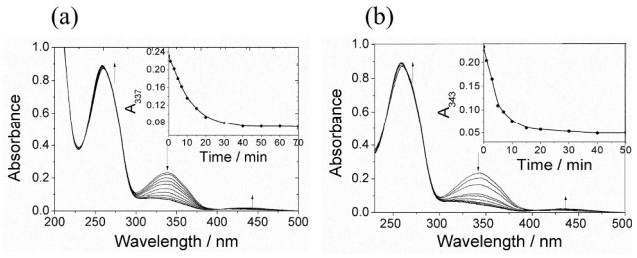

Figure 3. Absorbance change of **5a (a)** and **5b (b)** at maximum absorption of azobenzene as a function of UV irradiation time. UV experiments were performed in a 10 mM phosphate buffer (pH 7.0) containing 100 mM NaCl and 0.1 mM EDTA at room temperature. Concentrations of the ODNs were adjusted to 10 μM.

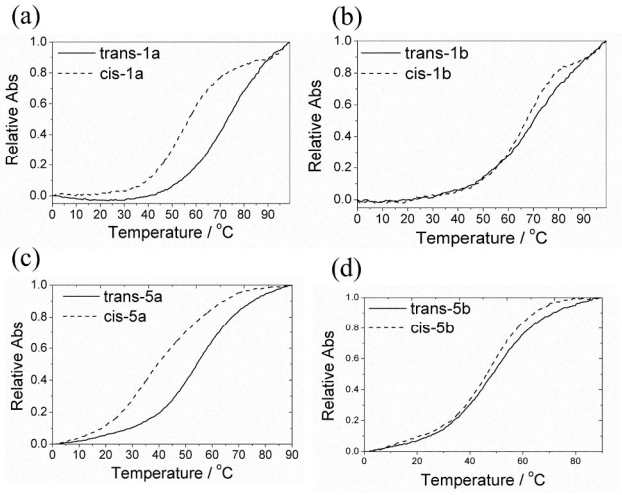

Figure 4. Comparison of normalized UV melting curves for trans-form (solid line) and cis form (broken line) of **1a (a)**, **1b (b)**, **5a (c)** and **5b (d)**. UV melting experiments were performed in a 10 mM phosphate buffer (pH 7.0) containing 100 mM NaCl and 0.1 mM EDTA. Concentrations of the ODNs were adjusted to 6 μM.

Photoregulation of stability of ODN hairpins by introducing azobenzene moiety

Typical melting curves of hairpin formation for **1a**, **5a**, **1b** and **5b** before or after UV irradiation were shown in Figure 4. These two curves of *trans* and *cis* form for **1a** and **5a** were sharply distinguished from each other with the large change of T_m, and the ΔT_m values of **1a** and **5a** were 18.4 °C and 18.9 °C respectively. In comparison, T_m values of *trans*-**1b** and *cis*-**1b** as well as *trans*-**5b** and *cis*-**5b** were almost identical and both ΔT_m were 2.6 °C, although two curves did not completely overlap. Similarly, other melting curves of modified ODN hairpin **1a-10a** and **1b-10b** were presented in Figure S7. Before and after UV light irradiation, the two melting curves were spread far apart for *trans*- and *cis*-**Az1** modified ODNs, whereas this did not occur for *trans*- and *cis*-**Az2** modified ODNs. The changes of T_m values of **1a-10a**, **1b-10b** induced by *trans* to *cis* isomerization were listed in Table 2. There was a decrease in T_m values at the range of 12.1 °C - 24.1 °C from *trans* and *cis* form of all **Az1**-ODN hairpins, while T_m values did not change from *trans*- and

Table 2. Comparison of T_m between *trans*-ODNs and *cis*-ODNs.[a]

Az1-ODN	ΔT_m[b]/°C	**Az2**-ODN	ΔT_m[b]/°C
1a	18.4	**1b**	2.6
2a	14.0	**2b**	1.2
3a	24.1	**3b**	1.0
4a	20.0	**4b**	1.8
5a	18.9	**5b**	2.6
6a	12.1	**6b**	-1.4
7a	15.0	**7b**	-6.2
8a	14.7	**8b**	-3.7
9a	17.3	**9b**	1.6
10a	13.9	**10b**	2.6

[a] The data were obtained by melting curve fitting and the values averaged by the different concentration range (2-120 μM). [b] $\Delta T_m = T_m$ (trans) $- T_m$ (cis).

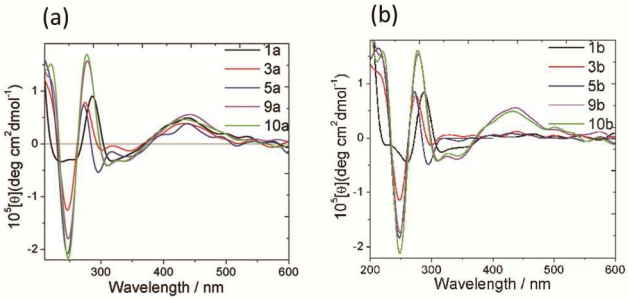

Figure 5. CD spectra of typical *trans*-Az1 ODNs **(a)** and *trans*-Az2 ODNs **(b)** in 10 mM phosphate buffer (pH7.0) containing 100 mM NaCl and 0.1 mM EDTA at 4 °C. Concentrations of the ODNs were 10 μM.

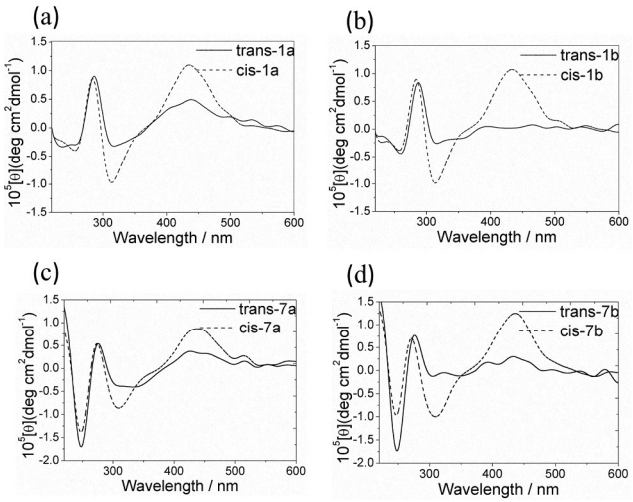

Figure 6. Comparison of CD spectra of *trans*-form (solid line) and *cis*-form (dash line) **1a (a)**, **1b (b)**, **7a,(c)** and **7b (d)** at 4 °C. CD spectra were measured in a 10 mM phosphate buffer (pH 7.0) containing 100 mM NaCl and 0.1 mM EDTA, the concentrations of DNAs were 10 μM.

cis-form of most **Az2**-ODN hairpins. Unexpectedly, T_m values of ODN **6b**, **7b** and **8b** were increased to different extent when *trans* ODNs were photoisomerized to their *cis* form. This could be attributed to formation of complex secondary structure from staggered A:T distribution.

CD spectra analysis of *trans*- and *cis*- ODNs

CD spectra of ODNs are sensitive to structure disturbances such as conformational change of azobenzene moiety and the distortion of base pairs. There were no CD signals for **Az1** and **Az2** linkers themselves due to absence of chiral centers, as shown in Figure S8. However, when **Az1** was incorporated in hairpins, CD signals at the range of 300-350 nm and 400-450 nm were observed for **1a**, **3a**, **5a**, **9a** and **10a** (Figure 5a). The induced CD signals could be caused by the interaction between azobenzene and neighbouring base pair. When **Az2** was incorporated in hairpins, **9b** and **10b,** having A:T base pair closing to azobenzene, displayed similar strong induced CD signals. Differently, **1b**, **3b** and **5b** with neighbouring G:C base pair, did not display CD signals at the range of 300-350 nm and 400-450 nm (Figure 5b). In addition, the induced CD signals for both **Az1**- and **Az2**-ODNs at the range of 300-350 nm and 400-450 nm become much stronger when *trans*-azobenzene were photoisomerized to *cis* form as shown as examples of **1a**, **1b**, **7a** and **7b** (Figure 6). There was similar increasing pattern from *trans* to *cis* state for other **Az1**-ODNs and **Az2**-ODNs (Figure S9). This result may be due to the factor that *cis*-form of azobenzene moiety in modified ODNs has more rigid structure than *trans*-form and could not rotate. Except for the induced CD of azobenzene linker, **Az1**-ODN **1a-10a** and **Az2**-ODN **1b-10b** had strong CD signals at the range from 240 to 300 nm, which was characteristic for the conformational information on the stem duplexes of ODNs. Based on CD signals with a positive peak near 275 nm and a negative valley centred at 240 nm, both *trans* and *cis* form of **Az1** and **Az2** ODNs adopted the B-form conformation.

Thermodynamic analysis of *trans*- and *cis*- hairpin ODNs

To obtain an insight into the stability regulation mechanism by photo-isomerization, we estimated thermodyamic parameters of azobenzene modified ODNs by a curve fitting method.[39, 40] Different from stilbene,[35] *cis*-azobenzene can retrieve to *trans*-form upon heating as well as visible-light irradiation. We first investigated the *cis* to *trans* conversion behaviour upon heating under the melting

Table 3. Comparison of thermodynamic parameters between *trans* form and *cis* form of **5a**, **6a**, **8a** and **5b**, **6b**, **8b**. [a]

Hairpin	T_m/°C	ΔG°_{37} (kcal/ mol)	ΔH° (kcal/ mol)	$T\Delta S^{\circ}$[b] (kcal/ mol)
trans-**5a**	54.2±0.1	-1.53±0.02	-29.08±0.51	-27.55±0.51
cis-**5a**	35.3±0.2	-0.002±0.02	-17.67±1.09	-17.67±1.11
trans-**5b**	49.9±0.5	-1.01±0.06	-24.45±1.46	-23.44±1.42
cis-**5b**	47.3±0.5	-1.05±0.01	-29.96±0.66	-28.92±0.6
trans-**6a**	56.7±0.2	-1.52±0.07	-26.40±0.67	-24.87±0.62
cis-**6a**	44.6±0.4	-0.66±0.03	-23.13±1.18	-22.47±1.15
trans-**6b**	56.5±0.6	-1.61±0.06	-26.66±0.70	-25.05±0.65
cis-**6b**	57.9±0.5	-1.97±0.11	-30.77±1.87	-28.80±1.76
trans-**8a**	46.6±0.3	-0.83±0.03	-26.40±0.2	-25.59±0.20
cis-**8a**	31.9±0.3	0.26±0.01	-20.43±0.62	-20.69±0.63
trans-**8b**	42.2±0.5	-0.45±0.01	-23.60±0.80	-23.15±0.81
cis-**8b**	45.9±0.3	-0.87±0.02	-26.67±0.33	-25.80±0.3

[a] Thermodynamic parameters were obtained by curve fitting method and the values averaged by the different concentration range (2-120 μM). [b] $T\Delta S^\circ = \Delta H^\circ(\text{ODN}) - \Delta G^\circ_{37}(\text{ODN})$.

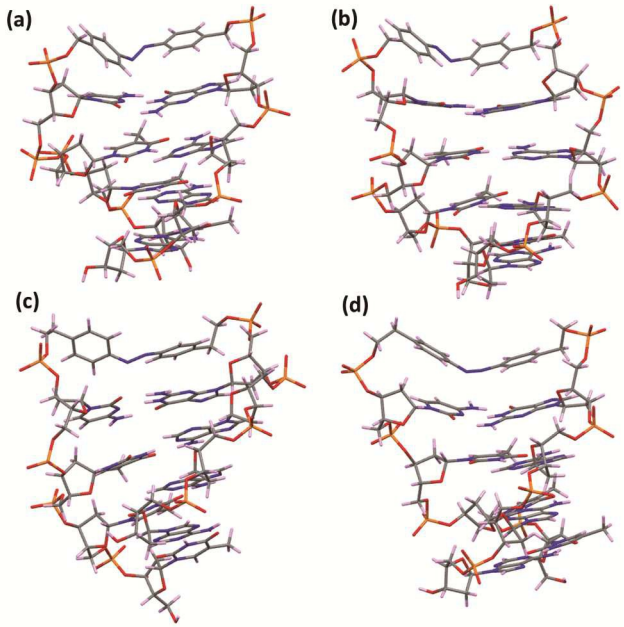

Figure 7. Views of the calculated structures of *trans*-**3a (a)**, *cis*-**3a (b)** *trans*-**3b (c)**, *cis*-**3b (d)** by molecular dynamic simulation.

experiments. UV melting curves of *cis*-azobenzene modified ODNs both at 260 nm and 350 nm were measured at a heating rate of 0.5 °C min^{-1}. In Figure S10, we found *cis*-**Az1** ODNs and *cis*-**Az2** ODNs started to transform to *trans*-form ODNs above 60 °C, which well agreed with the literature.[5] Therefore, thermodynamic parameters for hairpin formation of *trans*- and *cis*-state of **5a**, **5b**, **6a**, **6b**, **8a** and **8b** can be readily obtained due to the fact that their melting transitions occur over a narrow temperature range less than 60 °C, as listed in Table 3.

When *trans*-**Az1** photoisomerized to *cis* form, T_m values and free energies ($-\Delta G^o_{37}$) of **Az1**-ODN **5a**, **6a** and **8a** decreases as expected. Their enthalpic changes ($-\Delta H°$) for photoisomerization also significantly decreased by 11.41, 3.27 and 5.97 kcal/mol, respectively, while their entropic decreases ($-T\Delta S^o$) (9.88, 2.41, 4.88 kcal/mol) for **Az1**-ODN **5a**, **6a** and **8a** partially compensated the effect of their enthalpic changes. The relative lower stabilities of *cis*-**Az1** linked ODN **5a**, **6a** and **8a** were largely a consequence of less enthalpy. That is, the decrease of enthalpic change for photoisomerization was the primary driving force for effective destabilization of stem duplex of these ODNs, possibly due to the damage of hydrogen bond of the closing base pair or stacking interaction upon *trans* to *cis* isomerization. When *trans*-**Az2** isomerized to its *cis* form, the T_m values and free energies of ODN **5b**, **6b** and **8b** almost did not change. Instead, there was an increase in exothermicity ($-\Delta H°$) (5.51, 4.11 and 3.07 kcal/ mol) and entropic change (5.48, 3.75 and 2.65 kcal/ mol) for ODN **5b**, **6b** and **8b**. The result suggested that the consequence of enthalpy and entropy compensation bring about the similar free energy of hairpin formation for *trans*- and *cis*-**Az2** modified ODNs. A possible explanation for increasing enthalpy and entropic changes when *trans*-**Az2** was switched to its *cis*-isomer was that a relatively longer linker appeased steric repulsion of non-planar azobenzene.

A structural understanding will explain the stability regulation of azobenzene linked hairpin ODNs. The optimized structures of *trans*-**3a**, *cis*-**3a**, *trans*-**3b** and *cis*-**3b**, determined by molecular dynamics simulation and photoinduced conformational variations of azobenzene and its neighboring base pair were clearly shown in Figure 7. For **3a**, introduction of *trans*-azobenzene in the loop oligodeoxynucleotide did not affect the hydrogen bond interaction in hairpin stem. The neighboring base pair C:G showed that the lengths between H and O, N and H, O and H were 1.85, 1.91 and 1.81 Å, respectively, suggesting strong hydrogen bond interaction between the adjacent base pair.[41] Moreover, the *trans*-azobenzene can stack well with the adjacent base, although linking of stem bases in the hairpin affect planar structure of azobenzene. This may be taken from the fact that the centroid-centroid distance between base G and neighboring phenyl ring of azobenzene is 3.76 Å and their dihedral angles is 10.2°. On the other hand, azobenzene transforming from *trans* to *cis* with UV irradiation, the conformation changed to the more distorted structure, which moves base C far away from the neighboring phenyl ring of azobenzene moiety, and also enlarged centroid-centroid distance and the dihedral angles between base G and neighboring phenyl ring of azobenzene to 4.20 Å and 29.8°. It is previously reported that a strong π–π stacking interaction is quite often observed when the ring centroid contacts is below 3.8 Å as well as the displacement angle is less than 20°.[42] Thus, π–π stacking interaction between neighbouring base pair and azobenzene became weakened and even damaged when *trans* to *cis* isomerization of azobenzene moiety occurs, which led to *trans*-*cis* destabilization of azobenzene modified ODNs. In addition, the with the lengths of hydrogen bonds of H and O, N and H, O and H between neighboring base pair C:G (1.80, 1.91 and 1.83 Å, respectively) were seldom changed from *trans*-**3a** to *cis*-**3a**. For **3b**, the centroid-centroid distance between C/G and their corresponding neighbouring phenyl rings of azobenzene moiety is 4.83 and 3.42 Å, and the dihedral angle of plane G and corresponding phenyl ring was 3.7° in the *trans* state. Upon photoismerization from *trans* to *cis* azobenze, the centroid-centroid distance between C and G and their neighbouring phenyl ring of azobenzene is 4.83 and 3.47 Å, and the dihedral angle of plane G and corresponding phenyl ring was 1.6° in its *cis* state. In addition, the hydrogen bond lengths of C:G base pair between H and O, N and H, O and H were 1.78, 1.91, 1.82 Å in the *trans* state, and 1.82, 1.91, 1.83 Å in the cis state, respectively. The three bond lengths and π–π stacking interaction of azobenzene and base pair C:G for **3b** remained almost unchanged from *trans* to *cis* conformation probably due to the flexible longer linker unit, leading to the unchanged stability from *trans* to *cis*. Therefore, thermodynamic studies and theoretical calculation provided a solid theoretical basis for the our experimental observations that the stability of *trans*-form is much higher than its *cis*-form for **3a**, while *trans*- and *cis*-conformation of **3b** have similar stability.

Experimental Section

Synthetic procedure.

Synthesis and purification of azobenzene modified ODNs: azobenzene modified ODNs were prepared from the azobenzene phosphoramidite monomer **Az1** and **Az2** through solid DNA synthesizer using a program of 0.2 μM. All of the conventional 2'-deoxynucleotide phosphoramidite monomers, 3'-terminal nucleoside controlled pore glass support (CPG) and the reagents for DNA synthesis, were purchased from Glen Research Corporation and Wako Corporation. The modified ODNs were first treated with concentrated ammonium hydroxide at 55°C for 8 h, and then isolated as trityl-on derivatives and detritylated in 2% TFA by Sep-Pak column. HPLC purification of the sample solution was performed at 25 °C, and buffer (0.01 M TEAA, pH 7.0) and 50% MeOH (0.01 M

TEAA, pH7.0) mixture were used as gradient elution at a flow rate of 1.0 mL/min. Molecular weights were determined by means of were characterized by matrix-assisted laser desorption/ionization-time of flight mass spectrameter (MALDI-TOF-MS; ABI Voyager) using acetonitrile solution containing 50 mg anthranilic acid and 8 mg diammonium hydrogen citrate and 0.2% TFA solution as a matrix. The results were listed in the Table S1.

Photoisomerization of azobenzene modified oligonucleotides.

trans-cis photoisomerization was achieved with a UV lamp. The intensity of the UV light (Funakoshi 4 W handy UV lamp,) was below 0.4 J s^{-1} cm^{-2}. *cis-trans* photoisomerization was achieved with a daylight lamp. The sample solutions used as *cis*-ODNs were usually obtained after equilibrating by UV irradiation. 10 μM of sample solution in 10 mM phosphate buffer containing 100 mM NaCl and 0.1 mM Na_2EDTA was placed 5 mm away from the light source and irradiated at room temperature.

Measurement of melting temperatures and determination of thermodynamic parameters of azobenzene modified DNAs.

UV melting curves were measured in 10 mM phosphate buffer containing 100 mM NaCl and 0.1 mM Na_2EDTA by monitoring the absorbance at 260 nm, and the temperature ramp was 0.5 °C/min. The repeated melting curves for cooling and heating were virtually identical to each other. The T_m values were determined from the maximum in the first derivative of the melting curve. The changes in Gibbs free energy (ΔG^o_{37}) and the enthalpy change (ΔH^o) for the hairpin formation were determined by fitting the melting curves. The entropy changes ($T\Delta S^o$) at 37 °C were calculated from the ΔG^o_{37} and ΔH^o values of *trans*- and *cis*-conformation of azobenzene modified hairpins.[39, 40, 43]

Molecular dynamics simulation

MD simulation was performed with AMBER 11 molecular simulation package.[44] Ab initio quantum chemical methods were employed to obtain molecular mechanical parameters for Az1 and Az2 using the Gaussian 09 program.[45] The geometry was fully optimized and then the electrostatic potentials around them were determined at the HF/6-31G* level of theory. The RESP strategy[46] was used to obtain the partial atomic charges.

Starting models of studied *trans*-**3a**, *trans*-**3b**, *cis*-**3a**, and *cis*-**3b** were built using Discovery Studio 2.5 software.[47] All constructed molecules were solvated in TIP3P water using an octahedral box, of which extended 8 Å away from any solute atom. To neutralize the negative charges of simulated molecules, Na^+ counter ion was placed next to each phosphate group.

Molecular dynamics (MD) simulation was carried out by using the SANDER module of AMBER 11. The calculations began with 500 steps of steepest descent followed by 500 steps of conjugate gradient minimization with a large constraint of 500 kcal mol^{-1} $Å^{-2}$ on the solute atoms. Then 1000 steps of steepest descent followed by 1500 steps of conjugate gradient minimization with no restraints on the solute atoms were performed. Subsequently, after 20 ps of MD, during which the temperature was slowly raised from 0 to 300 K with weak (10 kcal mol^{-1} $Å^{-2}$) restraints on the solute atoms, the final unrestrained production simulations of 2.0 ns for all studied molecules were carried out at constant pressure (1 atm) and temperature (300 K). In the entire simulation, SHAKE was applied to all hydrogen atoms. Periodic boundary conditions with minimum image conventions were applied to calculate the nonbonded interactions. A cutoff of 10 Å was used for the Lennard-Jones interactions. The final structures of *trans*-**3a**, *trans*-**3b**, *cis*-**3a**, and *cis*-**3b** were produced from the 1,000 steps of minimized averaged structure of the last 1.0 ns of MD.

Conclusions

Az1 and **Az2** linkers were introduced to the loop position of hairpin ODNs with a variety of base-paired stems. The thermal stability of these ODNs is much higher than that of their corresponding natural ODNs due to the interaction between azobenzene and closing basepair. Photoisomerization of azobenzene unit was effectively performed and the thermal stability of hairpin ODNs was photoregulated for **Az1**-ODNs but not for **Az2**-ODNs. The difference in their photochemical behaviours is believed to depend on the linker unit between azobenzene and nucleobase. In addition, CD spectral analysis showed there were remarkably different characteristics for **Az2**-ODNs with G:C and A:T as neighbouring base pairs. For **Az1**-ODNs, the decrease of the thermostability due to *trans* to *cis* isomerization was also estimated by thermodynamic analysis. The results of dynamic simulations well agreed with stability photoswitching observed by experimental and thermodynamic analysis. Based on the photochemical results of **Az1**- and **Az2**-ODNs, **Az1** is an optimal linker unit for photoregulating thermostability of hairpin ODNs and can be applied in various ODN sequences, and thus possesses potential applications in biological systems and nucleic acid drugs as photoswitching of nucleic acid structures.

Acknowledgements

The work was funded by Chinese Nature Science Foundation (Grant No. 21302008, and Grant No.21272263), and The work was supported by State Key Laboratory of Natural and Biomimetic Drugs, Peking University (Grant No. K20140212 and Grant No. K20130206).

References

1. L. Wu, F. Pei, J. Zhang, J. Wu, M. Feng, Y. Wang, H. Jin, L. Zhang, X. Tang, *Chem Eur J* 2014, **20**,12114-12122.
2. L. Wu, Y. Wang, J. Wu, C. Lv, J. Wang, X. Tang, *Nucleic Acids Res* 2013, **41**,677-686.
3. X. Tang, *Photochemistry* 2013, **41**,319-341.
4. P. K. Jain, S. Shah, S. H. Friedman, *J Am Chem Soc* 2011, **133**,440-446.
5. L. Wu, K. Koumoto, N. Sugimoto, *Chem Commun* 2009, **45**,1915-1917.
6. X. Tang, J. Swaminathan, A. M. Gewirtz, I. J. Dmochowski, *Nucleic Acids Res* 2008, **36**,559–569.
7. P. Gorostiza, E. Y. Isacoff, *Science* 2008, **322**,395-399.
8. K. Takahashi, S. Yaegashi, H. Asanuma, M. Hagiya, *DNA computing* 2006, **3892**,336-346.
9. A. Nishikawa, S. Yaegashi, K. Ohtake, M. Hagiya, *DNA Computing* 2008, **48**,79-88.
10. Y. Kamiya, H. Asanuma, *Acc Chem Res* 2014, **47** 1663-1672.
11. F. Zhang, A. Zarrine-Afsar, M. S. Al-Abdul-Wahid, R. S. Prosser, A. R. Davidson, G. A. Woolley, *J Am Chem Soc* 2009, **131**,2283-2289.
12. Y. Kim, J. A. Phillips, H. Liu, H. Kang, W. Tan, *Proc Natl Acad Sci U S A* 2009, **106**,6489-6494.
13. J. Wu, X. Tang, *Bioorg Med Chem* 2013, **21**,6205-6211.
14. J. Wu, J. Wang, X. Tang, *Sci China Chem* 2014, **57**,322-328.
15. A. Kobori, T. Yamauchi, Y. Nagae, A. Yamayoshi, A. Murakami, *Bioorg Med Chem* 2012, **20**,5071-5076.
16. M. Op de Beeck, A. Madder, *J Am Chem Soc* 2012, **134**,10737-10740.
17. W. A. Velema, W. Szymanski, B. L. Feringa, *J Am Chem Soc* 2014, **136**,2178-2191.
18. J. Garcia-Amorós, D. Velasco, *Responsive Materials and Methods* 2014,27-58.

19. W. Szymanski, J. M. Beierle, H. A. Kistemaker, W. A. Velema, B. L. Feringa, *Chem Rev* 2013, **113**,6114-6178.
20. C. Garcı′ a-Iriepa, M. Marazzi, L. M. Frutos, D. Sampedro, *RSC Adv* 2013, **3**,6241-6266.
21. C. Dohno, K. Nakatani, *Chem Soc Rev* 2011, **40**.
22. C. Dohno, S. Uno, K. Nakatani, *J Am Chem Soc* 2007, **129**.
23. X. Wang, J. Huang, Y. Zhou, S. Yan, X. Weng, X. Wu, M. Deng, X. Zhou, *Angew Chem Int Ed* 2010, **49**,5305 -5309.
24. H. Asanuma, T. Takarada, T. Yoshida, X. Liang, M. Komiyama, *Angew Chem Int Ed* 2001, **40**,2671-2673.
25. T. Takarada, D. Tamaru, X. Liang, H. Asanuma, M. Komiyama, *Chem Lett* 2001, **30**,732-733.
26. X. Liang, H. Asanuma, M. Komiyama, *J Am Chem Soc* 2002, **124**,1877-1883.
27. H. Asanuma, X. Liang, H. Nishioka, D. Matsunaga, M. Liu, M. Komiyama, *Nature Protoc* 2007, **2**,203-212.
28. J. A. Phillips, H. Liu, M. B. O'Donoghue, X. Xiong, R. Wang, M. You, K. Sefah, W. Tan, *Bioconjugate Chem* 2011, **22**,282-288.
29. A. Aemissegger, V. Kräutler, W. F. van Gunsteren, D. Hilvert, *J Am Chem Soc* 2005, **127**,2929-2936.
30. S. Samanta, A. A. Beharry, O. Sadovski, T. M. McCormick, A. Babalhavaeji, V. Tropepe, G. A. Woolley, *J Am Chem Soc* 2013, **135**,9777-9784.
31. K. Yamana, A. Yoshikawa, H. Nakano, *Tetrahedron Lett* 1996, **37**,637.
32. K. Yamana, A. Yoshikawa, R. Noda, H. Nakano, *Nucleosides and Nucleotides* 1998, **17**,233.
33. K. Yamana, K. Kano, H. Nakano, *Bioorg Med Chem* 1999, **7**,2977.
34. Q. Wang, L. Yi, L. Liu, C. Zhou, Z. Xi, *Tetrahedron Lett* 2008, **49**,5087-5089.
35. F. D. Lewis, Y. Wu, X. Liu, *J Am Chem Soc* 2002, **124**,12165-12173.
36. F. D. Lewis, X. Liu, *J Am Chem Soc* 1999, **121**,11928-11929.
37. L. Duarte, R. Fausto, I. Reva, *Phys Chem Chem Phys* 2014.
38. A. A. Adamson, A. Vogler, H. Kunkely, R. Wachter, *J Am Chem Soc* 1978, **100**.
39. N. Sugimoto, S. Nakano, M. Yoneyama, K. Honda, *Nucleic Acids Res* 1996, **24**,4501-4505.
40. N. Sugimoto, S. K. Nakano, S., A. Matsumura, H. Nakamuta, T. Ohmichi, M. Yoneyama, M. Sasaki, 1995, **34**,11211-11216.
41. G. A. Jeffrey: An introduction to hydrogen bonding. In. Oxford University Press; 1997.
42. C. Janiak, *J Chem Soc, Dalton Trans,* 2000, **21**,3885-3896.
43. M. Petersheim, D. H. Turner, *Biochemistry* 1983 **22**,256-263.
44. D. A. Case, T. A. Darden, T. E. Cheatham, C. L. Simmerling, J. Wang, R. E. Duke, R. Luo, R. C. Walker, W. Zhang, K. M. Merz *et al*: AMBER **11**. In. San Francisco: University of California; 2010.
45. M. J. Frisch, G. W. Trucks, H. B. Schlegel, G. E. Scuseria, M. A. Robb, J. R. Cheeseman, G. Scalmani, V. Barone, B. Mennucci, G. A. Petersson *et al*: Gaussian 09, Revision A.1. In. Wallingford CT: Gaussian, Inc.; 2009.
46. C. I. Bayly, P. Cieplak, W. D. Cornell, P. A. Kollman, *J Phys Chem* 1993, **97**,10269-10280.
47. A. S. Inc.: Discovery Studio Modeling Environment. Release 2.5 ed. In. San Diego, CA: Accelrys Software Inc.; 2005.